

Original scientific article

<http://dx.doi.org/10.59456/afts.2023.1529.011T>

SMART MINING: JOINT MODEL FOR PARAMETRIZATION OF COAL EXCAVATION PROCESS BASED ON ARTIFICIAL NEURAL NETWORKS

Trivan Jelena¹, Kostić Srđan²

¹Faculty of Mining Prijedor, University of Banja Luka, Bosnia and Herzegovina,

e.mail: jelena.trivan@rf.unibl.org

²Faculty of Technical Sciences University of Novi Sad, Serbia, e.mail: srdjan.kostic@uns.ac.rs

ABSTRACT

In the present paper we propose a new artificial neural network model for the estimation of coal cutting resistance and excavator performance as a nonlinear relationship between the examined input (excavator movement angle in the left and right direction, slice height and thickness, coal unit weight, compressive and shear strength) and output factors (excavator effective capacity, maximum current/power/force/energy consumption, linear and areal cutting resistance). We analyze the dataset collected from three open-pit coal mines in Serbia: Field D, Tamnava Eastern Field and Tamnava Western Field (all part of the Kolubara coal basin). The model is developed using a multilayer feed-forward neural network, with a Levenberg-Marquardt learning algorithm. Results of the preformed analysis indicate satisfying statistical accuracy of the developed model ($R > 0.9$). Additionally, we analyze the individual effects of input factors on the properties of coal cutting resistance and performance of the excavator, by invoking the multiple linear regression. As a result, we single out the statistically significant and physically possible interactions between the individual controlling factors

Keywords: *artificial neural networks, surface coal mining, bucket wheel excavator*

INTRODUCTION

The rapid development of artificial intelligence (AI), its increased availability, and the possibility of use without having demanding processing units leads to the application of AI-based methods in almost every aspect of human activity. The main advantages of involving AI-based methods lie in their convenient use, satisfying accuracy and the essential black-box approach, i.e. one does not need to know all steps leading from input parameters to the outputs, but it is sufficient to repeat "experiments" with different settings of AI-based model in search of the best solution. Results obtained in this way are not always completely accurate, but their accuracy is satisfying for preliminary assessment of the processes or the features being studied. Regarding the mining industry, according to [forbes.com], AI-based methods lead to the so-called "smart mining", with the primary aim of reducing the enormous costs in the mining industry [1].

Regarding the mining industry, AI-based methods lead to the so-called "smart mining", with the primary aim of reducing the enormous costs in the mining industry [1]. For instance, estimations made by McKinsey [2] are that by 2035 the application of AI in mining will save between \$290 billion and \$390 billion annually for mineral raw materials producers. AI-based intelligence systems are being widely used by mining companies, helping them: acquire data, convert data, transmit, analyze, and visualize data. Moreover, Karatzoglou points out that future ore exploration will be more complex since

almost entire deposits that are on the surface or relatively easily accessible are nearly exhausted [3]. So, ore bodies that will explore in the future are likely to be deep and hidden by thick overburden, probably interacting with significant geological structures (including faults, and similar). In such cases, AI-based methods could be very useful, since they can "learn" from experience. Additionally, it is expected that the use of AI-based methods will increase the safety of the mine workers (by accurately predicting dangerous scenarios) and even lead to the use of autonomous mining vehicles, which could be remotely controlled and operated.

In the last decade, there has been an increased application of artificial intelligence methods in the planning, design, and analysis of processes and parameters related to the coal excavation process. Srivastava and Pradhan [4] reported that mining-related complex operations, computations, and analyses in India have become easier and more accurate with the use of AI-based methods. Wang et al. wrote about the "Chinese mode" of intelligent mining in underground coal mines [5].

The use of AI-based methods and solutions leads to the top-level architecture of 5G+ intelligent coal mine systems that combines intelligent applications such as autonomous intelligent mining, human-machine collaborative rapid tunneling, unmanned auxiliary transportation, closed-loop safety control, and intelligent ecology. Furthermore, according to Azhari et al. in the last five years, deep learning has been implemented to solve a variety of problems related to mine exploration, ore and metal extraction, and reclamation processes [6].

In coal mining, artificial neural networks (ANN) are by far the most used AI-based method in the last 10 years for solving different tasks in engineering practice. Yang and Xiaohong used artificial neural networks (ANN) to develop a quantitative prediction method for mining subsidence and horizontal movement under thin bedrocks and thick unconsolidated layers [7]. Results obtained indicated that the proposed model provides sufficiently accurate data when compared to the measured values, with a relative error in the range of 1.034 – 6.571% for subsidence, and 1.160 – 6.233% for horizontal movement.

Panigrahi and Ray used the ANN approach to develop a new electrochemical method (wet oxidation potential technique) for determining the susceptibility of coal to spontaneous combustion [8]. The model based on the ANN approach provided satisfying statistical accuracy, with $R > 0.9$ and $MSE = 0.66-2.07$ (target values were in the range 0-9). Mlynarczuk and Skiba used pattern recognition techniques and ANN to create an automatic process of classification of maceral groups and mineral components of coal [9]. Results obtained indicate over 97% of correct classifications of maceral groups and mineral components.

Wilkins et al. applied convolutional neural networks to identify microseismic events at the coal mine [10]. The developed model could be used to reveal, classify and locate microseismic events, with satisfying precision. Moreover, their research indicated that the created model was more successful than humans at correctly identifying both true events and false-positive events.

Jiang et al. used graph convolutional networks to develop a multi-point relationship fusion prediction model of mining-induced surface subsidence, based on the surface deformation data obtained from 250 InSAR images [11]. Qi et al. applied a radial basis function neural network for the estimation of the spatial distribution of soil organic carbon in coal mining subsidence areas [12]. Results obtained indicate that the application of neural networks provides statistically more accurate results compared to direct kriging methods (correlation coefficient 0.81 compared to 0.44, respectively).

In the present paper, we apply a three-layer feedforward multiple perceptron neural network, to estimate a series of parameters of the bucket-wheel excavator performance and coal cutting resistance. The model is derived for the case study of three coal basins in Serbia: Tamnava western field, Tamnava eastern field, and Field D (all parts of the Kolubara coal basin). As a result, the model provides an estimation of many excavation and resistance parameters with satisfying accuracy, and it could be used for the first preliminary assessment of excavator consumption and coal resistance to cutting.

The paper is structured as follows. In Section 2 we provide brief information on the data analyzed and applied methodology. In Section 3 results of the performed analysis are presented, including the estimation of the statistical accuracy of the developed model and the explicit mathematical expression. Section 4 is devoted to the conclusions and directions for further research.

DATA ANALYZED AND METHODOLOGY

We analyze the following properties of the excavation process (using a bucket-wheel excavator) recorded at Tamnava Eastern Field, Tamnava Western Field, and Field D (Kolubara coal mine in Serbia):

- Excavator effective capacity Q_{ef} (m³/h)
- maximum current consumption I_{max} (A)
- maximum power consumption N_{max} (kW)
- maximum force consumption P_{max} (kN)
- maximum energy consumption E_{max} (kWh/m³)
- excavator movement angle in the left direction φ_L (°)
- excavator movement angle in the right direction φ_D (°)
- slice height h (m)
- slice thickness s (m)

Also, the following properties of coal are examined:

- maximum linear cutting resistance K_{Lmax} (N/cm)
- maximum areal cutting resistance K_{Fmax} (N/cm²)
- coal unit weight γ (kN/m³)
- coal compressive strength σ_p (MPa)
- coal cohesion c (MPa)
- coal angle of internal friction φ (°)

Data were collected [13] for the case of coal excavation with a bucket-wheel excavator of the same type SchRs630.

The aforementioned data were further used to develop a prediction model, as a nonlinear function of the following output units: Q_{ef} , I_{max} , N_{max} , P_{max} , E_{max} , K_{Lmax} , and K_{Fmax} , on the following controlling factors: γ , σ_p , c , φ , φ_L , φ_D , h and s . ANN approach included a fast-forward three-layer network with a backpropagation Levenberg-Marquardt (LM) algorithm with a sigmoid activation function. The LM learning algorithm is the fastest method for training moderate-sized feed-forward neural networks. We develop an ANN model with 10 hidden neurons (Figure1).

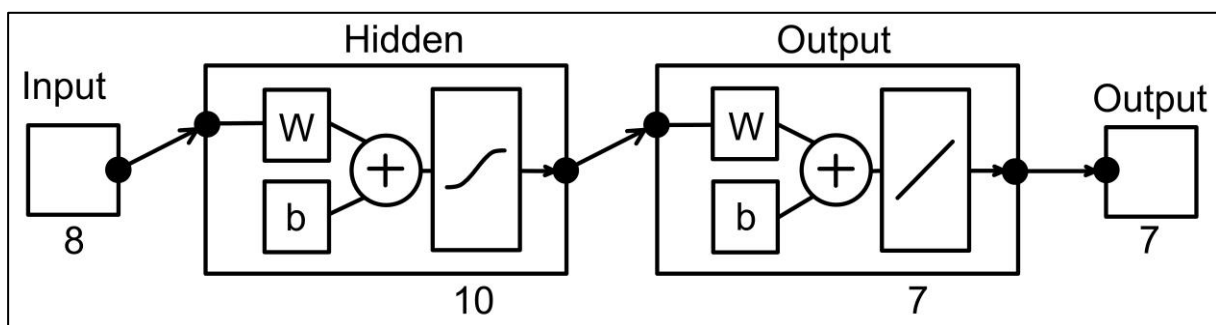


Figure 1. The architecture of the developed ANN model.

The possibility of overfitting was excluded by confirming that any increase in accuracy over the training data set yields a rise in accuracy over a validation data set. In particular, mean-squared error (MSE) should be saturated with the increase of epochs for training and validation data. The total data set has been divided as follows: 65% for training (128 recordings), 20% for validation (40 recordings), and 15% for testing (30 recordings).

DEVELOPMENT OF ANN MODEL

As a result, we developed a unique ANN model, by establishing a nonlinear correlation between the outputs Q_{ef} , I_{max} , N_{max} , P_{max} , E_{max} , K_{Lmax} , and K_{Fmax} , and inputs: γ , σ_p , c , ϕ , ϕ_L , ϕ_D , h and s , in the following general form:

$$[outputs] = tansig\{[a] + [b] \cdot tansig\{[c] + [d] \cdot [input]\}\} \tag{1}$$

where $tansig[N]$ is a neural transfer function, that takes a matrix of net input vectors, N , and returns the S-by-Q matrix, A , of the elements o N squshed into $[-1 \ 1]$. It is defined as:

$$tansig(N) = \frac{2}{1+e^{-2N}} - 1 \tag{2}$$

and it is mathematically equivalent to $\tanh(N)$.

Parameters of Eq. (1) are given as matrices in the present case:

$$[outputs] = \begin{bmatrix} Q_{ef} \\ I_{max} \\ N_{max} \\ P_{max} \\ E_{max} \\ K_{Lmax} \\ K_{Fmax} \end{bmatrix}, [a] = \begin{bmatrix} -1.90 \\ 0.26 \\ -0.53 \\ 0.61 \\ -0.39 \\ 1.25 \\ 0.08 \end{bmatrix}, [c] = \begin{bmatrix} -0.810 \\ 0.067 \\ 1.488 \\ -0.272 \\ 1.342 \\ 0.839 \\ -2.319 \\ 0.961 \\ 2.743 \\ 1.895 \end{bmatrix},$$

$$[b] = \begin{bmatrix} 0.05 & -0.05 & -1.080 & 0.139 & 0.651 & 1.718 & -0.659 & 0.783 & 1.847 & 0.597 \\ -0.06 & 0.018 & 0.033 & 0.337 & 1.775 & -0.150 & -0.291 & -0.608 & 1.227 & -0.105 \\ 0.003 & -0.018 & -0.146 & -0.071 & 0.108 & -0.040 & -0.064 & 0.206 & 0.459 & -0.889 \\ -0.23 & 0.336 & 0.544 & -0.239 & -1.204 & -0.317 & 0.150 & -0.175 & -1.015 & -1.030 \\ 0.41 & 0.048 & -0.079 & 0.587 & -0.306 & -0.113 & -0.380 & -0.324 & 0.334 & -1.035 \\ 0.06 & 0.160 & -0.128 & -0.485 & 1.240 & -0.034 & 0.171 & 0.015 & 0.845 & -1.552 \\ 0.09 & -0.236 & 0.156 & 0.020 & -0.490 & -0.306 & 0.283 & 0.120 & -1.502 & 0.572 \end{bmatrix}, \text{ and}$$

$$[d] = \begin{bmatrix} 2.968 & -0.629 & -1.964 & -1.398 & -0.793 & 1.124 & 0.868 & -1.806 \\ 2.347 & 1.141 & -0.658 & -2.514 & 1.158 & -1.487 & 1.165 & -0.969 \\ -0.499 & -0.225 & 0.966 & -0.922 & -0.487 & 0.289 & 1.272 & -0.254 \\ 0.305 & -0.155 & 1.475 & 0.429 & 1.199 & -1.020 & 1.218 & -1.031 \\ -0.357 & 0.338 & 0.934 & -0.029 & 0.172 & -0.074 & 2.953 & 0.016 \\ -0.309 & -0.333 & -0.131 & -0.522 & -0.621 & 0.966 & 1.611 & 0.015 \\ -0.327 & -0.129 & 0.485 & -0.717 & -0.532 & 0.981 & 1.124 & -2.415 \\ 0.215 & 1.701 & 1.571 & -0.660 & 0.647 & -1.260 & -1.067 & 0.022 \\ 0.852 & -1.023 & 0.539 & -0.115 & 1.322 & 1.149 & -2.729 & 1.871 \\ 0.959 & 2.373 & -1.941 & -0.287 & 0.939 & 0.005 & -1.214 & -0.128 \end{bmatrix}.$$

Developed model (1) provides statistically accurate results, as shown in Figure 2. In all phases of model development, satisfying estimation accuracy was achieved with a correlation coefficient higher than 0.9. The distribution of residuals is given in Figure 3. According to different normality tests, residuals do not follow a normal distribution, Figure 4. Results of the runs test ($p < 0.05$) also indicate the absence of randomness in the analyzed data.

The possibility of overfitting was excluded by confirming that any increase in accuracy over the training data set yields a rise in accuracy over a validation data set. In Figure 5. we plot the gradient values, μ , and validation fail. The values of gradient, μ , and val fail were 10^{-7} , 10^{10} , and 6 at 15 epochs, respectively, indicating that the ANN model was well-trained.

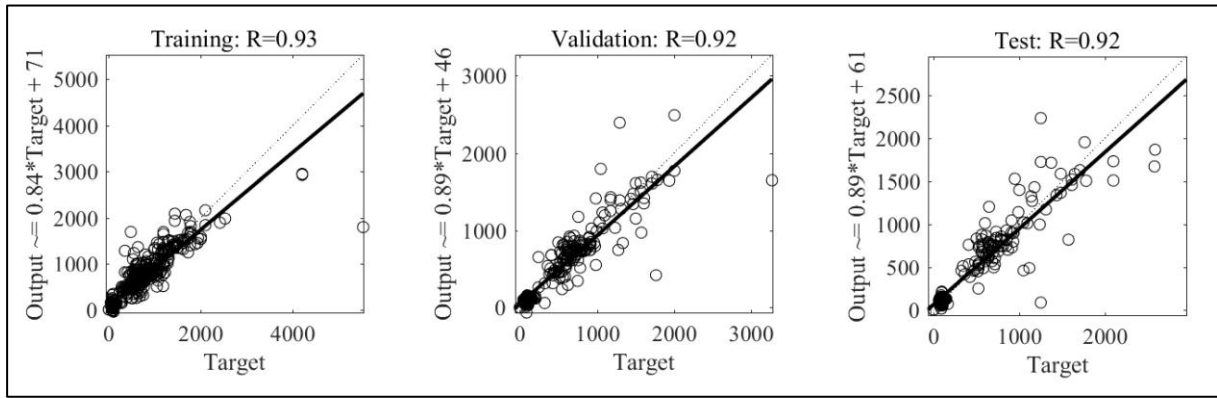


Figure 2. Regression plots for model (1): (left) training set, (middle) validation set, (right) testing set.

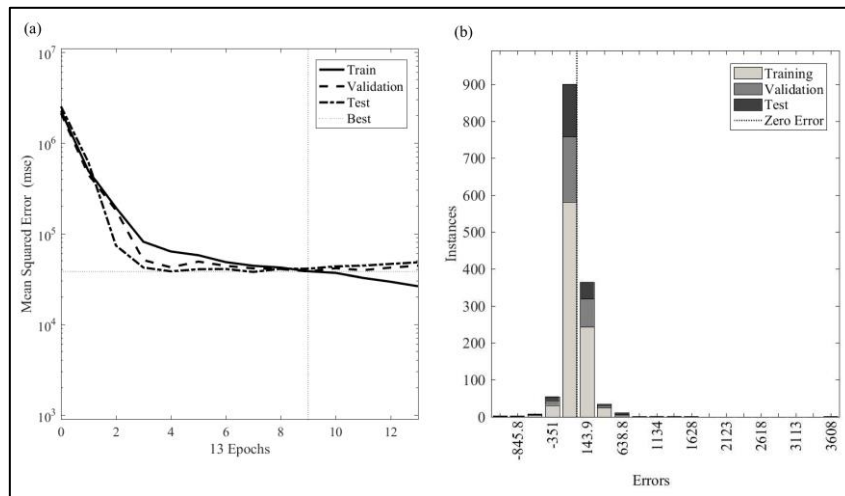


Figure 3. (a) Training evaluation for development of model (1), (b) distribution of residuals of model (1).

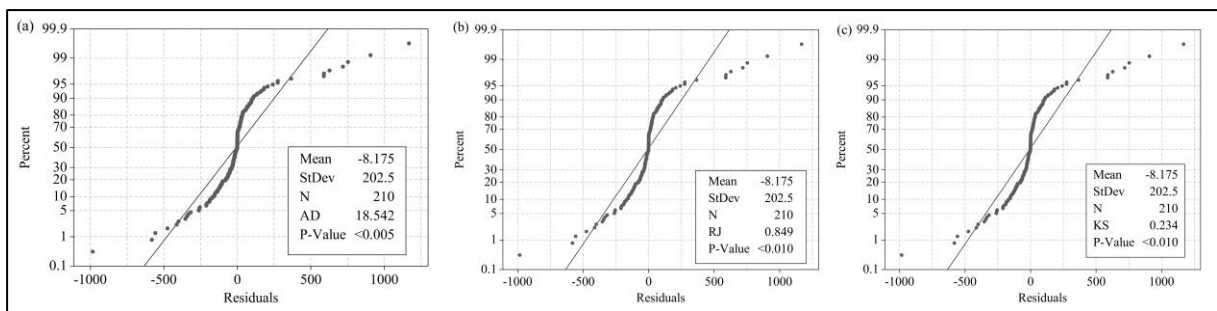


Figure 4. Results of normality tests for residuals: (a) Anderson-Darling test, (b) Ryan-Joiner test, (c) Kolmogorov-Smirnov test.

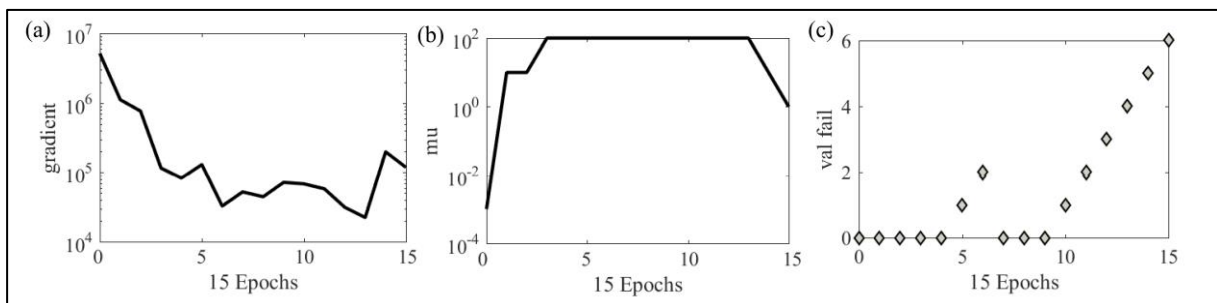


Figure 5. (a) Gradient values, (b) mu and (c) validation fail for the trained ANN model.

INDIVIDUAL EFFECTS OF INPUT FACTORS

The effect of input factors on each output unit is assessed by invoking the multiple linear regression method. Explicit mathematical expressions are provided in Tables 1-2.

Table 1. Statistically significant individual factors and two-factor interactions on Q_{ef} , N_{max} , P_{max} , and E_{max} .

ln (Q_{ef})		1/(N_{max})		Sqrt (P_{max})		ln (E_{max})	
0.008	γ	-3.6E-05	γ	0.29	γ	-0.05	γ
-7.52	σ_p	0.000237	σ_p	-31.69	σ_p	0.039	σ_p
-0.26	φ	-0.00308	c	54.36	c	-3.5	c
-0.12	φ_L	-1.8E-05	φ_L	0.26	φ_L	-0.004	φ
0.0007	φ_D	4.37E-05	φ_D	-0.31	φ_D	0.026	φ_L
-0.81	h	-0.00177	s	18.7	h	-0.022	φ_D
5.05	s	-0.00064	$\sigma_p \times s$	-7.65	s	0.132	h
0.14	$\sigma_p \times \varphi$	0.00046	c x h	-0.037	$\sigma_p \times \varphi_L$	0.167	$\gamma \times s$
0.019	$\sigma_p \times \varphi_L$	4.57E-05	$\varphi \times s$	0.041	$\sigma_p \times \varphi_D$	-0.379	$\sigma_p \times s$
-0.363	$\sigma_p \times \varphi_D$	5.85E-08	$\varphi_L \times \varphi_D$	2.18	$\sigma_p \times s$	0.0002	$\varphi_L \times \varphi_D$
-0.037	c x φ_L	1.03E-05	$\varphi_D \times s$	0.02	$\varphi_L \times h$	-0.008	$\varphi_D \times s$
0.0014	$\varphi \times \varphi_L$			-0.015	$\varphi_D \times h$	0.52	* h * s
-0.0002	$\varphi_L \times \varphi_D$			4.15	σ_p^2		
				0.45	s ²		

Table 2. Statistically significant individual factors and two-factor interactions on I_{max} , K_{Lmax} , and K_{Fmax} .

ln (I_{max})		ln(K_{Lmax})		ln (K_{Fmax})	
2.66	γ	0.39	γ	0.39	γ
-3.06	σ_p	5.99	c	-0.126	φ
-0.29	c	0.073	φ_L	0.07	φ_L
1.81	φ	-0.052	φ_D	-0.026	φ_D
-0.05	φ_L	-2.15	s	1.27	h
0.05	φ_D	-0.001	$\sigma_p \times \varphi_L$	-0.013	$\sigma_p \times \varphi_L$
3.45	s	0.0086	$\sigma_p \times \varphi_D$	0.01	$\sigma_p \times \varphi_D$
-1.43	$\gamma \times c$	-0.53	c x h	-2.40	c x s
0.01	$\sigma_p \times \varphi_L$	0.0039	$\varphi_L \times h$	0.005	* Fi L * h
-0.01	$\sigma_p \times \varphi_D$	-0.0045	$\varphi_D \times h$	-0.007	* Fi D * h
1.11	c x h	-0.005	$\varphi_D \times s$	-0.007	* Fi D * s
-0.09	$\varphi \times h$	0.26	* h * s	0.447	* h * s
-0.18	h x s	0.26	σ_p^2	-0.161	h ²
0.33	σ_p^2	0.16	s ²		
5.68	c ²				
-0.019	φ^2				
-0.00005	φ_L^2				
-0.18	s ²				

Statistically significant individual factors affecting Q_{ef} are presented in Figure 6. One can clearly single out two groups of parameters (input factors) that have different effects on Q_{ef} , Figure 6:

- slice thickness has the most significant predominant influence on Q_{ef} . It is expected that the increase in slice height will lead to an increase in Q_{ef} .
- minor effect comes from the following group of parameters:
 - unit weight, compression strength, and cohesion have qualitatively the same effect, which could be described as a minor positive (increasing) influence, meaning that the increase of these parameters leads to the increase of Q_{ef} .

- Slice height and excavator movement angle in right and left directions have minor, but negative (decreasing) effects on Q_{ef} , meaning that the increase of these parameters leads to a decrease in Q_{ef} .

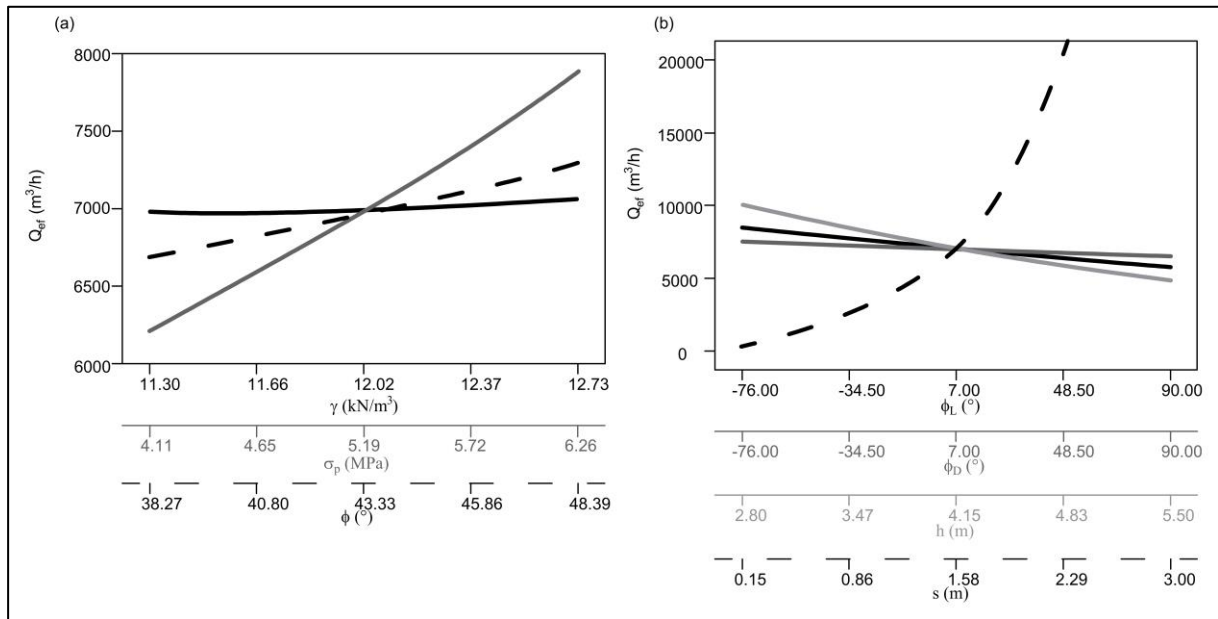


Figure 6. Effect of individual factors on Q_{ef} : (a) Q_{ef} as a function of γ , σ_p and ϕ ; (b) Q_{ef} as a function of ϕ_L , ϕ_D , s and h . While a single parameter is varied, others are held at constant moderate values: $\gamma = 12.02$ kN/m³, $c = 1.25$ MPa, $\phi_L = 7^\circ$, $\phi_D = 7^\circ$, $h = 4.15$ m, $s = 1.58$ m, $\sigma_p = 5.19$ MPa, $\phi = 43.33^\circ$.

Regarding the individual effects of input factors on I_{max} , three groups of parameters could be singled out, Figure 7:

- Parameters with significant predominant positive (increasing) influence on I_{max} : σ_p and c .
- Parameters with minor negative (decreasing) influence on I_{max} : γ , ϕ_D .
- Parameter with minor positive (increasing) influence on I_{max} : s , ϕ_L , ϕ

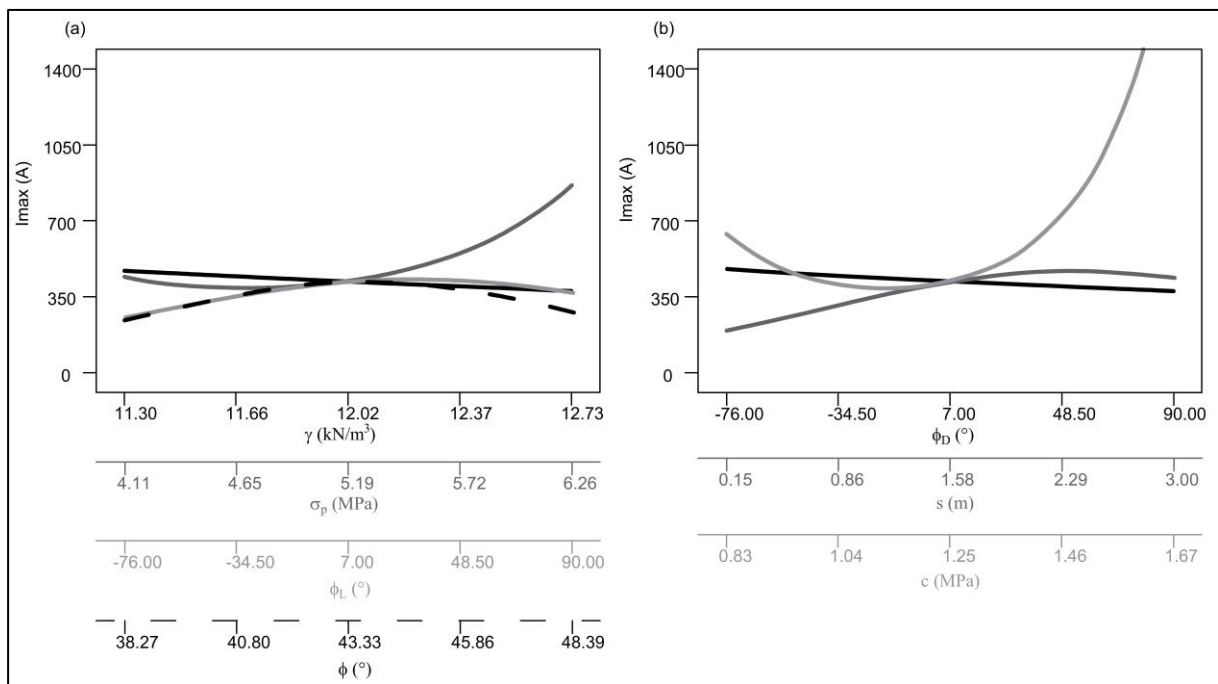


Figure 7. Effect of individual factors on I_{max} : (a) I_{max} as a function of γ , σ_p , ϕ_L , and ϕ ; (b) I_{max} as a function of ϕ_D , s , c , and h . While a single parameter is varied, others are held at constant moderate values: $\gamma = 12.02$ kN/m³, $c = 1.25$ MPa, $\phi_L = 7^\circ$, $\phi_D = 7^\circ$, $h = 4.15$ m, $s = 1.58$ m, $\sigma_p = 5.19$ MPa, $\phi = 43.33^\circ$.

The examined input factors have the following effects on N_{max} , Figure 8:

- Unit weight has almost no effect on N_{max} .
- Compression strength and cohesion have a significant positive (increasing) effect on N_{max} .

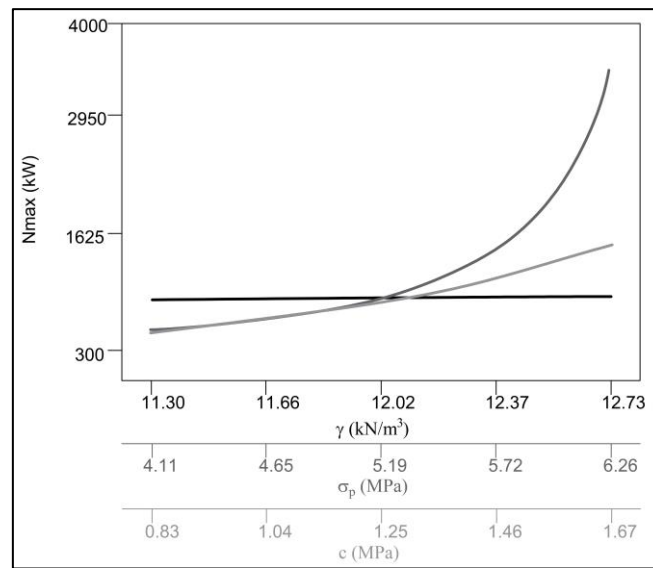


Figure 8. Effect of individual factors on N_{max} : γ , σ_p , and c . While a single parameter is varied, others are held at constant moderate values: $\gamma = 12.02$ kN/m³, $c = 1.25$ MPa, $\phi_L = 7^\circ$, $\phi_D = 7^\circ$, $h = 4.15$ m, $s = 1.58$ m, $\sigma_p = 5.19$ MPa, $\phi = 43.33^\circ$.

Regarding the dependence of P_{max} on the analyzed input factors, the results of the analysis indicate the following, Figure 9:

- Slice height and coal unit weight have a minor positive effect on P_{max} .
- Slice thickness s and angle of the excavator movement in the left direction have a strong positive (increasing) effect on P_{max} .
- Excavator movement angle in the right direction has a strong negative (decreasing) effect on P_{max} .
- Compression strength and coal cohesion have negative effects for the lower range of values. For the upper range of values, they have a positive (increasing) effect.

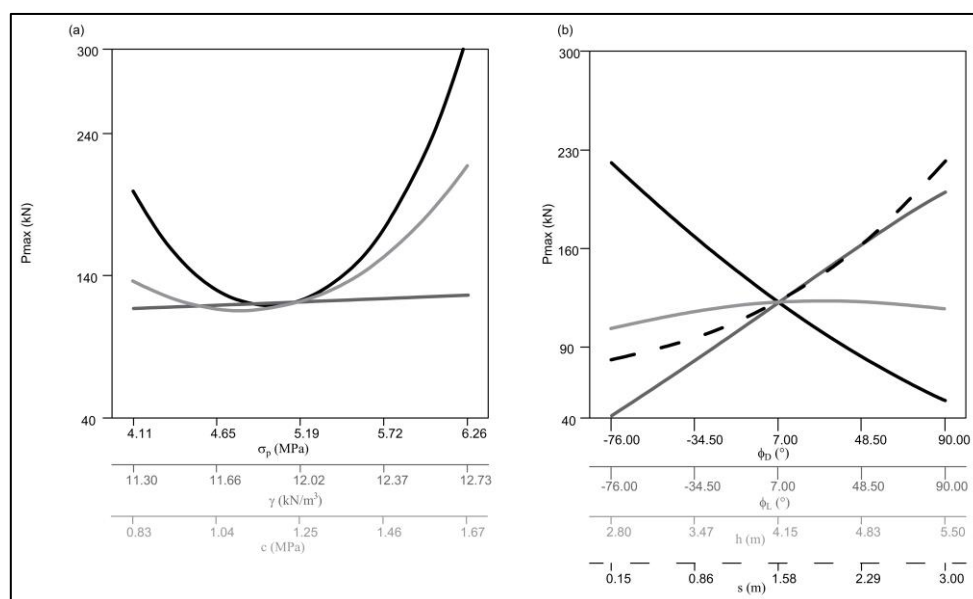


Figure 9. Effect of individual factors on P_{max} : (a) P_{max} as a function of γ , σ_p , and c ; (b) P_{max} as a function of ϕ_D , ϕ_L , h , and s . While a single parameter is varied, others are held at constant moderate values: $\gamma = 12.02$ kN/m³, $c = 1.25$ MPa, $\phi_L = 7^\circ$, $\phi_D = 7^\circ$, $h = 4.15$ m, $s = 1.58$ m, $\sigma_p = 5.19$ MPa, $\phi = 43.33^\circ$.

Results of the performed analyses indicate the following influence of the input factors on E_{max} , Figure 10:

- Coal unit weight, compression strength, cohesion, and friction angle have almost no effect on E_{max} ;
- Excavator movement in the left direction and slice height have a slight positive (increasing) effect on E_{max} ;
- Excavator movement in the right direction has a slight negative (decreasing) effect on E_{max} .

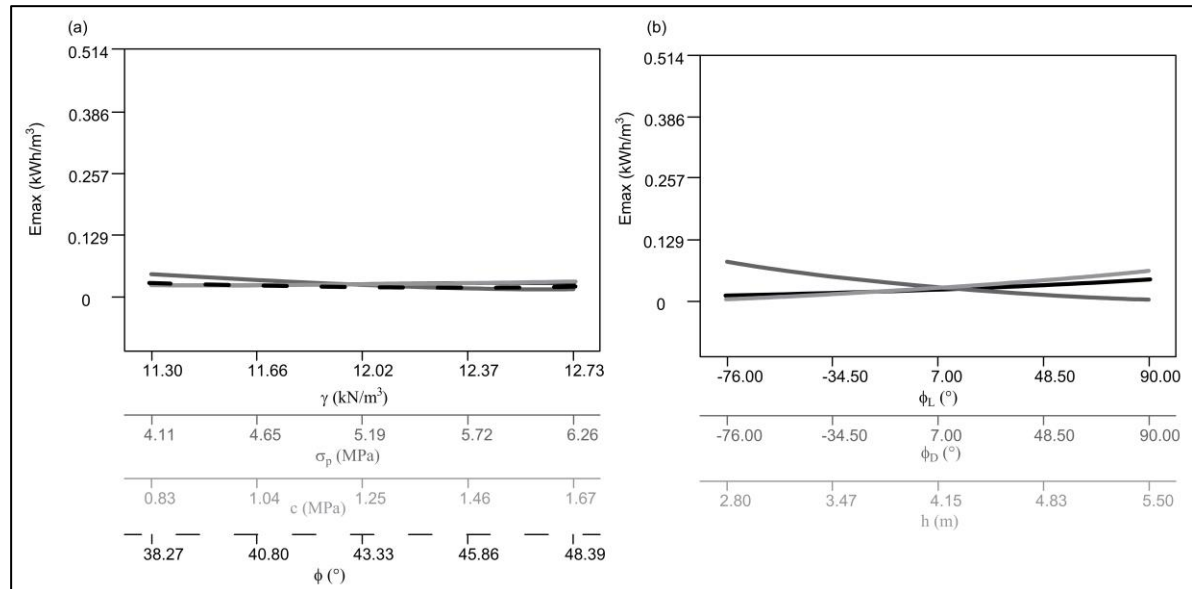


Figure 10. Effect of individual factors on E_{max} : (a) E_{max} as a function of γ , σ_p , c and ϕ ; (b) E_{max} as a function of ϕ_D , ϕ_L , and h . While a single parameter is varied, others are held at constant moderate values: $\gamma = 12.02$ kN/m³, $c = 1.25$ MPa, $\phi_L = 7^\circ$, $\phi_D = 7^\circ$, $h = 4.15$ m, $s = 1.58$ m, $\sigma_p = 5.19$ MPa, $\phi = 43.33^\circ$.

The dependence of K_{Lmax} on the input factors is the following, Figure 11:

- Coal unit weight, cohesion, excavator movement angle in the left direction, and slice height have a slight positive (increasing) effect on K_{Lmax} ;
- Excavator movement in the right direction has a significant negative (decreasing) effect on K_{Lmax} ;

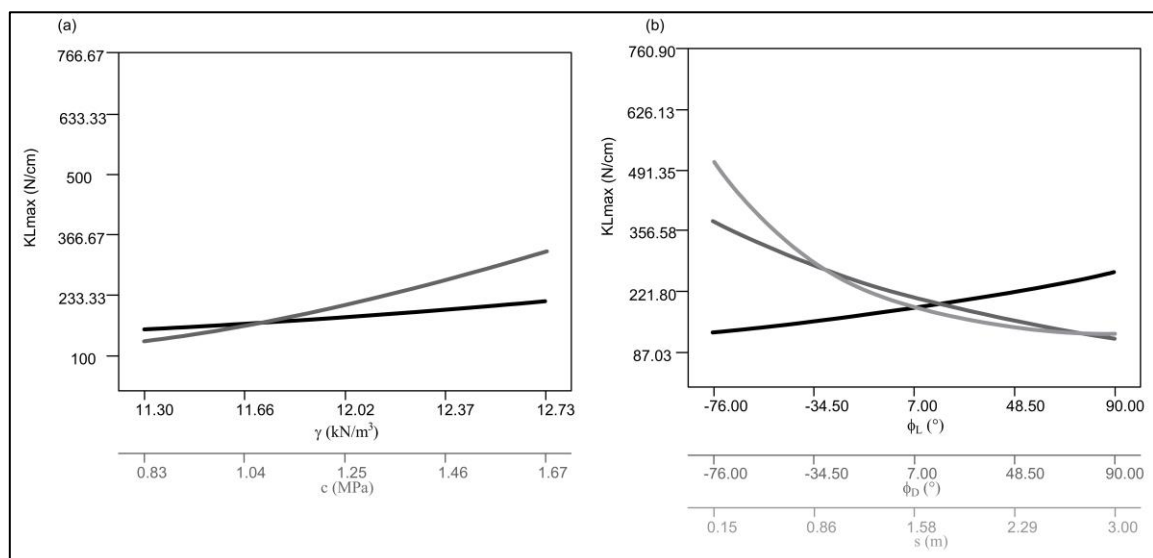


Figure 11. Effect of individual factors on K_{Lmax} : (a) K_{Lmax} as a function of γ and c ; (b) K_{Lmax} as a function of ϕ_D , ϕ_L , and s . While a single parameter is varied, others are held at constant moderate values: $\gamma = 12.02$ kN/m³, $c = 1.25$ MPa, $\phi_L = 7^\circ$, $\phi_D = 7^\circ$, $h = 4.15$ m, $s = 1.58$ m, $\sigma_p = 5.19$ MPa, $\phi = 43.33^\circ$.

Obtained results indicate the following effect of the examined input factors on K_{Fmax} , Figure 12:

- Excavator movement angle in either direction and coal friction angle have almost no effect on K_{Fmax} ;
- Coal unit weight has a minor positive (increasing) effect on K_{Fmax} , which is the expected impact;
- Slice height has a significant positive (increasing) effect on K_{Fmax} , which is also expected;

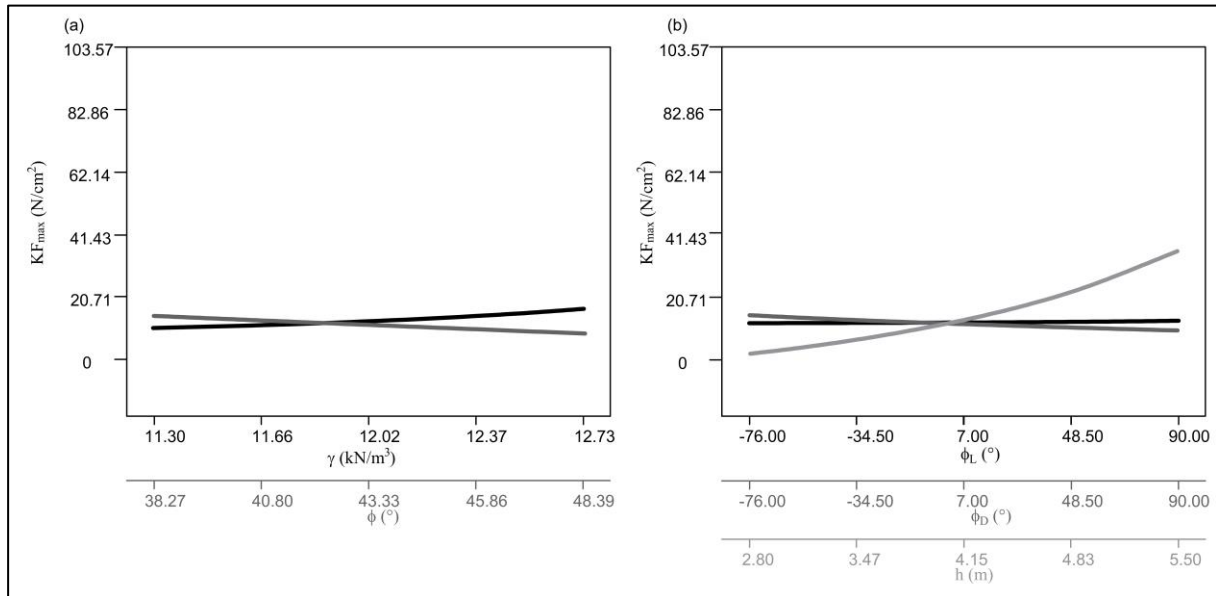


Figure 12. Effect of individual factors on K_{Fmax} : (a) K_{Fmax} as a function of γ and ϕ ; (b) K_{Fmax} as a function of ϕ_D , ϕ_L and h . While a single parameter is varied, others are held at constant moderate values: $\gamma = 12.02 \text{ kN/m}^3$, $c = 1.25 \text{ MPa}$, $\phi_L = 7^\circ$, $\phi_D = 7^\circ$, $h = 4.15 \text{ m}$, $s = 1.58 \text{ m}$, $\sigma_p = 5.19 \text{ MPa}$, $\phi = 43.33^\circ$.

CONCLUSIONS

In the present paper, we propose a new model for the estimation of coal cutting resistance and excavator performance based on the application of artificial neural networks. The developed model includes the following input parameters: slice height h (m), slice thickness s (m), coal unit weight γ (kN/m^3), coal compressive strength σ_p (MPa), coal cohesion c (MPa), and coal angle of internal friction ϕ ($^\circ$), and the following output parameters: excavator effective capacity Q_{ef} (m^3/h), maximum current consumption I_{max} (A), maximum power consumption N_{max} (kW), maximum force consumption P_{max} (kN), maximum energy consumption E_{max} (kWh/m^3), excavator movement angle in the left direction ϕ_L ($^\circ$), and excavator movement angle in the right direction ϕ_D ($^\circ$), maximum linear cutting resistance K_{Lmax} (N/cm) and maximum areal cutting resistance K_{Fmax} (N/cm^2).

Statistical analysis of the obtained results indicates high statistical reliability of the developed model, with $R > 0.92$. In contrast to our previous research [14], where we invoked the deep neural network approach, here we apply a multilayer perceptron feed-forward neural network, which results in the explicit mathematical expression for estimation of coal cutting resistance and excavator performance that could be further used in engineering practice.

Additionally, in the present paper, we provide a detailed analysis of the effect of statistically significant and physically possible individual factors on the examined output factors. In particular, the results of our analysis indicate the following:

- Effect of slice height h :
 - minor, but negative (decreasing) effect on Q_{ef} ,
 - minor positive effect on P_{max} ,
 - a slight positive (increasing) effect on E_{max} ,
 - a slight positive (increasing) effect on K_{Lmax} ;
 - a significant positive (increasing) effect on K_{Fmax} .

- Effect of slice thickness s :
 - the most significant predominant influence on Q_{ef} ,
 - a strong positive (increasing) effect on P_{max} .
- Effect of excavator movement angle in the left direction φ_L ($^\circ$)
 - minor, but negative (decreasing) effect on Q_{ef} ,
 - a strong positive (increasing) effect on P_{max} ,
 - a slight positive (increasing) effect on E_{max} ;
 - a slight positive (increasing) effect on K_{Lmax} ,
 - almost no effect on K_{fmax} .
- Effect of excavator movement angle in the right direction φ_D ($^\circ$)
 - minor, but negative (decreasing) effect on Q_{ef} ,
 - a strong negative (decreasing) effect on P_{max} ,
 - a slight negative (decreasing) effect on E_{max} ,
 - a significant negative (decreasing) effect on K_{Lmax} .
- Effect of coal unit weight γ (kN/m^3)
 - minor positive (increasing) influence on Q_{ef} ,
 - almost no effect on N_{max} ,
 - minor positive effect on P_{max} ,
 - almost no effect on E_{max} ,
 - a slight positive (increasing) effect on K_{Lmax} ,
 - a minor positive (increasing) effect on K_{Fmax} .
- coal compressive strength σ_p (MPa)
 - minor positive (increasing) influence on Q_{ef} ,
 - significant positive (increasing) effect on N_{max} ,
 - negative effect on P_{max} for the lower range of values; for the upper range of values there is a positive (increasing) effect on P_{max} ,
 - almost no effect on E_{max} .
- coal cohesion c (MPa)
 - minor positive (increasing) influence on Q_{ef} ,
 - significant positive (increasing) effect on N_{max} ,
 - negative effect on P_{max} for the lower range of values; for the upper range of values there is a positive (increasing) effect on P_{max} ,
 - almost no effect on E_{max} ,
 - a slight positive (increasing) effect on K_{Lmax} .

The coal friction angle has almost no influence on any of the examined output factors.

The presented approach and developed model could be further utilized for smart planning of open-pit coal mining and optimization of the excavation process. The performance of the developed model could be improved and made for general use if a larger dataset is examined in the succeeding studies.

Received September 2023, accepted November 2023)

REFERENCES

- [1] <https://www.forbes.com/sites/cindygordon/2021/07/31/ai-innovations-in-mining/?sh=72466dee4ec0>
- [2] <https://www.prescouter.com/2020/08/smart-mining-how-artificial-intelligence-can-benefit-the-mining-industry/>
- [3] Bui, X., Bui, H., Nguyen, H. (2020). A Review of Artificial Intelligence Applications in Mining and Geological Engineering. Proceedings of the International Conference on Innovations for Sustainable and Responsible Mining. Part of the Lecture Notes in Civil Engineering book series (LNCE, volume 109)
- [4] Shrivastava P., Pradhan, G.K. (2022). Use of Artificial Intelligence in Mining: An Indian Overview. International Congress and Workshop on Industrial AI 2021. Part of the Lecture Notes in Mechanical Engineering book series (LNME).
- [5] Wang, G., Ren, H., Zhao, G., Zhang, D., Wen, Z., Meng, L., Gong, S. (2022). Research and practice of intelligent coal mine technology systems in China. International Journal of Coal Science & Technology 9:24.

- [6] Azhari, F., Sennersten, C., Lindley, C., Sellers, E. 2023. Deep learning implementations in mining applications: a compact critical review. *Artificial Intelligence Review* <https://doi.org/10.1007/s10462-02310500-9>
- [7] Yang, W., Xiaohong, X. (2013). Prediction of mining subsidence under thin bedrocks and thick unconsolidated layers based on field measurement and artificial neural networks. *Computers and Geosciences*, 52, 199 – 203.
- [8] Panigrahi, D.C., Ray, S.K. (2014). Assessment of self-heating susceptibility of indian coal seams - A neural network approach. *Archives of Mining Sciences* 59, 4, 1061 – 10761.
- [9] Mlynarczuk, M., Skiba, M. (2017). The application of artificial intelligence for the identification of the maceral groups and mineral components of coal. *Computers and Geosciences*, 103, 133 – 141.
- [10] Wilkins, A., Strange, A., Duan, Y., Luo, X. (2020). Identifying microseismic events in a mining scenario using a convolutional neural network. *Computers and Geosciences*, 137, 104418.
- [11] Jiang, B., Zhang, K., Liu, X., Lu, Y. (2023). Prediction model with multi-point relationship fusion via graph convolutional network: A case study on mining-induced surface subsidence. *PLoS ONE*, 18, 8, e0289846.
- [12] Qi, Q., Yue, X., Duo, X., Xu, Z., Li, Z. (2023). Spatial prediction of soil organic carbon in coal mining subsidence areas based on RBF neural network. *International Journal of Coal Science and Technology*, 10, 1, 30.
- [13] Ignjatović, D. (2003). Study on optimization of the construction of buckets of the bucket-wheel excavator in order to increase the capacity of the excavator. University of Belgrade Faculty of Mining and Geology (In Serbian), pp. 218. doi: [10.1371/journal.pone.0289846](https://doi.org/10.1371/journal.pone.0289846)
- [14] Kostić, S., Stojković, M., Ilić, V., Trivan, J. (2023). Deep Neural Network Model for Determination of Coal Cutting Resistance and Performance of Bucket-Wheel Excavator Based on the Environmental Properties and Excavation Parameters. *Processes* 11, 3067. <https://doi.org/10.3390/pr11113067>